JACS
JOURNAL OF THE AMERICAN CHEMICAL SOCIETY

COMMUNICATION

pubs.acs.org/JACS

Spontaneous Formation and Characterization of Silica Mesoporous Crystal Spheres with Reverse Multiply Twinned Polyhedral Hollows

Lu Han,[†] Ping Xiong,[‡] Jingfeng Bai,[‡] and Shunai Che*[,†]

[†]School of Chemistry and Chemical Engineering, State Key Laboratory of Metal Matrix Composites, Shanghai Jiao Tong University, 800 Dongchuan Road, Shanghai 200240, P. R. China

[‡]Biomedical Instrument Institute of Shanghai Jiao Tong University, 1954 Huashan Road, Shanghai 200030, P. R. China

Supporting Information

ABSTRACT: A crystal is an object with translational symmetry. Basic research into and production of new materials necessitates the preparation of crystals of a particular morphology and with well-defined crystal defects. In this work, we found novel silica mesoporous crystal spheres with polyhedral hollows (icosahedral, such as those observed for proteins of virus capsids, decahedral, Wulff polyhedral, etc.) formed by the reverse multiply twinned bicontinuous double diamond mesostructure. Vesicles with a low-curvature lamellar structure were first formed by the self-assembly of amphiphilic carboxylic acid molecules in the presence of a nonionic surfactant and then underwent a structural transformation process that gave a reverse multiply twinned mesoporous shell while maintaining the hollow shape. These polyhedral hollow crystals showed an enhanced contrast of backscattering signatures relative to the incident acoustic signals and thus could be used as a potential contrast agent in medical ultrasonography with drug loadings in the mesopores.

Morphologies and crystallographic structures are believed to be the key of crystal properties, and control of crystalline materials at the mesoscopic level is one of the most challenging issues faced by synthetic chemists. There is growing interest in the preparation of hollow structures because of their potential applications in catalysis, controlled drug release, artificial cells, light fillers, and photonic crystals.[1] Some anisotropic hollow inorganic nanostructures with regular morphologies have been prepared through various synthetic strategies.[2]

Silica mesoporous crystals (SMCs), which can be considered as "cavity crystals", were discovered in the early 1990s.[3] SMCs can be formed on surfactant micelles that act as templates for the self-assembly and subsequent and/or simultaneous condensation of inorganic precursors.[4] Extensive research has resulted in SMCs with a variety of ordered structures[5] and morphologies.[6] Hollow SMCs (HSMCs) have also been prepared using various templating routes, with the aim of using them in adsorption, chromatography, drug delivery, catalysis, etc.[7] Occasionally, HSMCs having a spherical outer shape and a hexagonal hollow with a shell exhibiting two-dimensional hexagonal *p6mm* symmetry have been observed.[8]

Herein we report novel HSMCs exhibiting an extraordinary polyhedral hollow with inner facets formed by a reverse multiply twinned bicontinuous double diamond mesoporous shell, which has not previously been observed in crystal structures. These HSMCs show an excellent echoing characteristic with respect to incident acoustic signals. The HSMCs were synthesized using amino acid-derived, anionic, amphiphilic *N*-stearoyl-L-glutamic acid (C_{18}GluA) as the template, 3-aminopropyltrimethoxysilane (APS) as a costructure directing agent (CSDA), and tetraethyl orthosilicate (TEOS) as the silica source in the presence of the nonionic surfactant $C_{16}H_{31}(OCH_2CH_2)_{10}OH$ (Brij-56). The amino group of the CSDA interacts electrostatically with the negatively charged headgroup of the anionic amphiphilic molecules, while the alkoxysilane site cocondenses with the silica source to form the silica framework.[9]

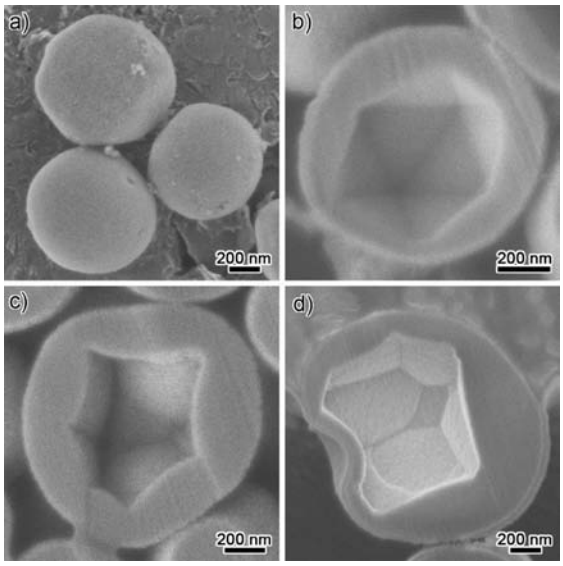

Figure 1. Morphology of the HSMCs. (a) SEM image of the calcined HSMCs, showing their spherical shape. (b−d) Cross-sectional images of HSMCs, showing various inner morphologies.

Figure 1a shows scanning electron microscopy (SEM) images of HSMCs synthesized with C_{18}GluA:Brij-56:APS:TEOS:H_2O = 1:1.45:2:15:2335. The HSMCs have a well-defined spherical morphology with diameters from 600 nm to 2 μm, although most of the HSMCs are less than 1 μm in diameter. After cross-section polishing, which uses a beam of accelerated argon ions to polish the material, the unusual polyhedral hollows were clearly revealed. The icosahedral hollow, in which each vertex is shared by

Received: November 20, 2010
Revised: March 29, 2011
Published: April 06, 2011

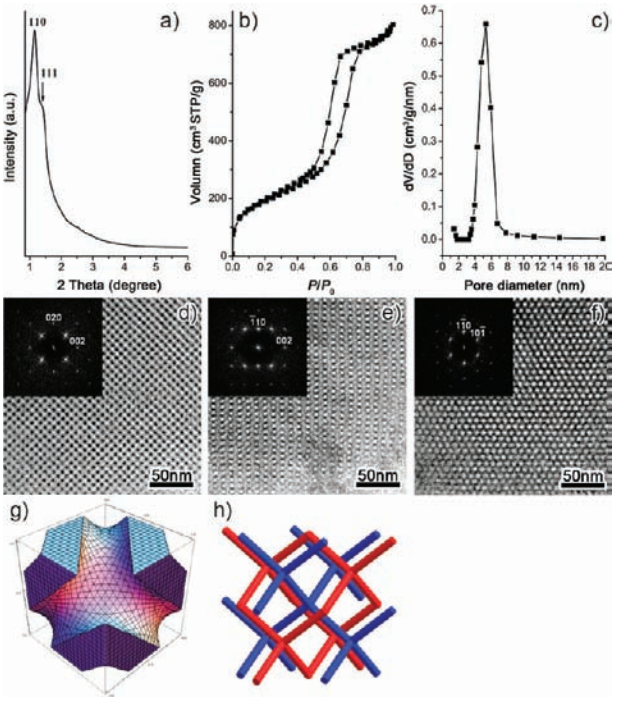

Figure 2. Shell structure of the HSMCs. (a) XRD pattern of the calcined HSMCs with Cu Kα1 radiation (λ = 1.5406 Å). (b) Nitrogen adsorption−desorption isotherms. (c) Pore size distribution as determined by a Barrett−Joyner−Halenda (BJH) plot of the derivative of the pore volume per unit weight with respect to the pore diameter (dV/dD), based on the desorption branch. (d−f) HRTEM images and corresponding FDs taken along the (d) [100], (e) [110], and (f) [111] directions. (g) 3D reconstruction of one unit cell along the [111] direction. (h) Schematic representation of the double diamond structure.

five faces and has fivefold symmetry, was often observed (Figure 1b). For the relevant observed shapes, other types of polyhedra in which each vertex is shared by three or four faces could also be categorized (Figure 1c,d). More SEM images are provided in Figure S1 in the Supporting Information.

The powder XRD pattern of the HSMCs (Figure 2a) shows an intense reflection with a shoulder in the range $1° < 2\theta < 2°$ and a d spacing ratio of about $\sqrt{3}/\sqrt{2}$, which can be indexed to 110 and 111 reflections of the cubic unit cell, as confirmed later by high-resolution transmission electron microscopy (HRTEM). The unit cell parameter was found to be a = 10.8 nm. N_2 adsorption−desorption analysis of the HSMCs revealed a typical type-IV isotherm with an evident hysteresis loop in the range $0.5 < P/P_0 < 0.8$ (Figure 2b). The Brunauer−Emmett−Teller (BET) surface area and single-point total pore volume of the material were measured as 688.5 $m^2 g^{-1}$ and 1.24 $cm^3 g^{-1}$, respectively. The pore diameter was ~5.3 nm. The mesostructure of the shell was checked by HRTEM by crushing the sample into small pieces. The HRTEM images taken along the [100], [110], and [111] directions are shown in Figure 2d−f. The Fourier transform diffractograms (FDs) showed the following reflection conditions: *hkl*, none; *0kl*, $k + l$ = even; *hhl*, none; *00l*, l = even. From these results, two space groups are possible: $Pn\bar{3}$ (No. 201) or $Pn\bar{3}m$ (No. 224). The space group $Pn\bar{3}m$ was chosen because of its high symmetry. An electron crystallography study (Figure 2g,h; see the Supporting Information for details) showed the mesostructure to be composed of two disconnected but interwoven tetrahedrally connected networks divided by a silica wall grown along a typical diamond minimal surface (D surface).[10]

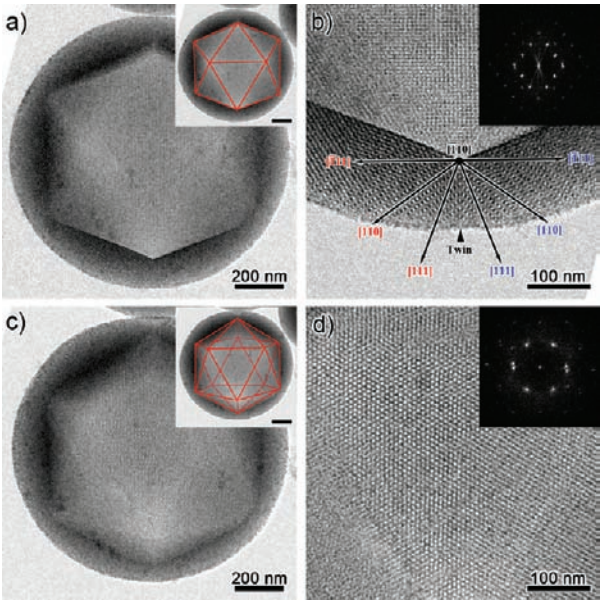

Figure 3. HRTEM images of an HSMC with an icosahedral hollow. (a) TEM image taken from the intersection edge of two triangles; the inset shows a structural model. (b) Magnified TEM image of the twin plane in (a). (c) TEM image taken from the center of a triangle, with a structural model shown in the inset. (d) Magnified TEM image of the center in (c).

Figure 3 shows TEM images at different tilting angles for a crystal with an icosahedral hollow inside. The thickness contrast clearly presents the inner morphology. Figure 3a shows the TEM image taken through the center of two opposite intersection edges, clearly showing the twofold symmetry of the icosahedron. Interestingly, a twin structure was observed at the boundary of the two domains taken from the common $[\bar{1}10]$ direction (Figure 3b). The $[\bar{1}11]$, [110], and [111] directions are in the same plane perpendicular to the $[\bar{1}10]$ direction, and they differ by 35.3° from each other. It can be clearly seen that the inner facet is (111). When the crystal was tilted toward the center of a triangle, threefold symmetry was observed (Figure 3c,d), and the magnified HRTEM image of the center area shows the typical ⟨111⟩ contrast. Therefore, all of the domains are interconnected via a shared (111) surface and form an icosahedral shape, and the inner surface consists of 20 {111} faces. This is the first observation that a twin can be formed in bicontinuous minimal surface structures (also see Figure S2).

A decahedral hollow was also observed (Figure 4a,b). The entire crystal gave 10-fold symmetry in its diffraction patterns, as did the quasi-crystals, and the twin structures were clearly observed. On the basis of the TEM contrast and the structural model, a model of a fivefold center was constructed (Figure 4b inset). The five twins meet along a common [110] direction, and all of the inner planes are {111}. We predict that the vertexes of the icosahedral shape shown in Figure 3 also follow this arrangement. Single crystals were also observed. Figure 4c,d is a TEM image of a crystal taken from the [100] direction. It shows a truncated octahedron (a so-called Wulff polyhedron) enclosed by eight {111} and six {100} facets. Moreover, other inner morphologies, combinations of single-crystal and multiply twinned parts, were also observed. Thus, the morphologies shown in Figure 1c,d can be explained by hollows enclosed by only {111} facets (decahedron or octahedron) and by both {111} and {100} facets (Wulff polyhedra), respectively.

The exceptional morphologies included herein can be explained by the formation of reverse multiply twinned particles

dx.doi.org/10.1021/ja110443a | J. Am. Chem. Soc. 2011, 133, 6106–6109

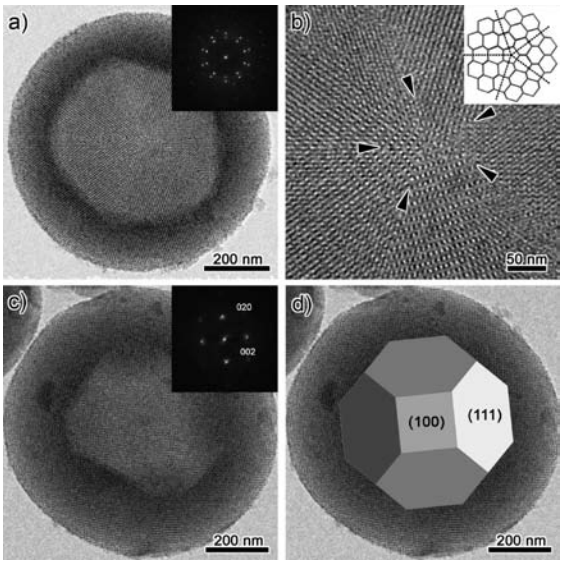

Figure 4. HRTEM images of HSMCs with decahedral and Wulff polyhedral hollows. (a) TEM image taken from the common [110] direction of the decahedron shape. (b) Magnified TEM image of the center area in (a). The inset shows a structural model of the fivefold center. (c) TEM image of a Wulff polyhedron taken from the [100] direction. (d) TEM image overlaid with the Wulff polyhedron model.

(MTPs). The MTP model was first introduced in the 1960s by Ino,[11] and it successfully explains the presence of the icosahedral or decahedral shape of metal particles. For a face-centered cubic (fcc) crystal, the surface energies (γ) of the low-index crystallographic facets follow the order $\gamma\{111\} < \gamma\{100\} < \gamma\{110\}$, suggesting that a single crystal should take an octahedral or tetrahedral shape to maximize the exposure of {111} facets. However, a single crystal normally evolves into a Wulff polyhedron with a nearly spherical shape, which has the smallest surface area, in order to minimize the total interfacial free energy. However, MTPs can be also formed by achieving the lowest total free energy by maximizing the surface coverage with {111} facets.[12] Recently, MTPs have been found in fcc SMCs.[13] Since SMCs are much more flexible before the completion of silica polymerization, they can compensate for the internal strain energy caused by the angular misfits (the tetrahedral angle is 109.5°, and the angle of a pentagon is 108°) during the formation of the MTPs.

The MTPs and pentagonal structures have also been discovered in the germanium structure, which has a diamond cubic structure.[14] In this kind of structure, the valence bonds are assumed to be flexible enough to generate an angular misfit. In our case, the reverse MTPs formed by the double diamond structure follow a rule similar to that for the germanium structure. However, it is the first observation of such hollow MTP crystals, which are not icosahedra or decahedra obtained by the packing of tetrahedrons sharing {111} facets but rather polyhedral hollows with inner facets formed by reverse MTP structures.

To investigate the morphological and structural evolution of the HSMCs, the XRD patterns, TEM and SEM images of the products originating from the same initial mixture were monitored as a function of reaction time (Figures S3−S5). After APS and TEOS were added to the surfactant solution, the XRD pattern of the products sampled before 1 h showed a lamellar structure with two reflections having a *d*-spacing ratio of 2/1. After 1 h, the two reflections in the 2θ range of 1−2° with a *d*-spacing ratio of $\sqrt{3}/\sqrt{2}$ began to grow at the expense of the lamellar peaks as a result of the formation of the double diamond mesostructure. SEM and TEM images showed that the aggregated hollow architectures were formed at the very early stage of the reaction (stirred for 10 min). The aggregated spheres then became separated with the structural transformation. The existence of polyhedral hollows after 12 h indicates the completion of the structural and morphological transformation.

These results indicate that the HSMCs were formed by a lamellar-to-cubic shell transformation of vesicles. The influence of the nonionic surfactant on mesostructures is associated with the surfactant packing parameter $g = V/a_0 l$, where V is the chain volume, a_0 is the effective hydrophobic/hydrophilic interfacial area, and l is the chain length (see the Supporting Information for details).[15] The cloud point of Brij-56 is in the range 64−69 °C,[16] and its hydrophobicity could be increased with increasing temperature due to the destruction of the hydrogen bond between Brij-56 and H_2O. Therefore, at higher temperatures, the highly hydrophobic Brij-56 tends to be associated with the hydrophobic part of the surfactant, which increases the hydrophobic volume of the micelle and favors low organic/inorganic interface curvature with a large value of the *g* parameter. On the other hand, SMC nanoparticles can easily be formed by addition of the block copolymer P123 ($EO_{20}PO_{70}EO_{20}$) or Brij-56;[17] this is considered to be achieved by the effective dispersion of the nucleation sites of the SMCs by nonionic surfactants. Therefore, the lamellar-structured vesicles were formed by packing of Brij-56 molecules on the surfactant and the dispersion effect.

However, the formation of SMCs with a complex form is not an equilibrium process, and it normally involves growth and transformation.[18] In this system, vesicles with a lamellar structure underwent a structural transformation to the double diamond mesostructure. The driving force seems to be the silica condensation, which causes the negative charge density of the silicate network to decrease. The enhanced interaction between the CSDA and the surfactant would drive the silica close to the micelle surface, and the organic surfactants would then pack to form a higher surface curvature. Stacked hexagonal arrays of fusion channels within the surfactant bilayers would be formed first and then rearrange to form the double diamond structure (Figure S6).[19] It is worth noting that $[111]_{cubic}$ is perpendicular to the lamellar layer, facing the center of the sphere, which induced the reverse MTP. The exterior surface was kept as spherical, perhaps to minimize the surface free energy by forming the globular shape in the synthesis mixture. The formation of the polyhedral hollow may be a general phenomenon during the formation of the hollow shell when the synthesis proceeds in two steps, initial hollow architecture formation and subsequent recrystallization or structural transformation to highly ordered structures. The hollow morphology is determined by the point-group symmetries[8] or unique properties such as the MTP in our case. Thus, precise design and control of the synthesis conditions is necessary.

It is well-known that gas bubbles and polymer hollow spheres have been widely used as contrast agents in ultrasonography on the basis of the compressibility and density differences between the agent and blood.[20] It was considered that the reflection planes of the polyhedral hollow shape may provide a larger scattering cross section for the ultrasound wave, which would provide stronger backscattered signatures formed by the outer surface and enhanced by the hollow. Here we found that the HSMCs work as an outstanding contrast agent to enhance the backscattered signatures from incident ultrasound signals. Figure 5 shows an in vitro ultrasound image of HSMCs obtained by

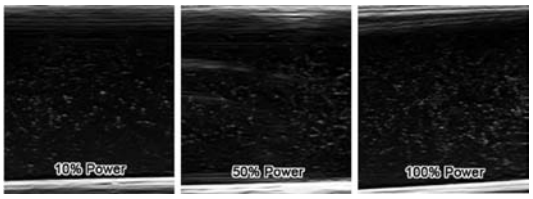

Figure 5. In vitro ultrasound images of HSMCs (33 μg/mL) in degassed aqueous solution with a 7 MHz transducer.

linear ultrasound imaging (B-model). It can be clearly observed that HSMCs have a superior response to the ultrasound with various particle sizes even at low emission power (see Figures S7 and S8 for details). While hollow silica spheres have recently been suggested for use as contrast agents because of their high biocompatibility and mechanical stability,[21] there have been no reports that SMCs have been used in ultrasonography. Notably, HSMCs are an ideal reservoir for storage and controlled drug release and thus could be used as a potential therapy-detection unified material for medical treatment. The data reported here represent only initial work; detailed mechanistic studies and further experiments are underway.

In this work, we have synthesized novel HSMCs with remarkable reverse MTP polyhedral hollows. The exceptional crystal structure and unique properties open a new avenue in crystallographic and materials research that might have a significant impact on crystal engineering, materials science, and mineralogy. The formation process provides a new method to generate hollow materials with designed structure and morphology by structural transformation or recrystallization of the initially formed hollow architecture. The echoing characteristic of the HSMCs may also open a new direction in pharmacy and ultrasonography studies.

■ ASSOCIATED CONTENT

Supporting Information. Experimental procedures, SEM and TEM images, electron crystallographic analyses, and results of time-course and ultrasound experiments. This material is available free of charge via the Internet at http://pubs.acs.org.

■ AUTHOR INFORMATION

Corresponding Author
chesa@sjtu.edu.cn

■ ACKNOWLEDGMENT

The authors thank Prof. Osamu Terasaki for cooperation and discussion. We acknowledge the support of the National Natural Science Foundation (Grant 20890121), the 973 Project (2009CB930403), and the Grand New Drug Development Program (2009ZX09310-007) of China. The microscopy works were supported by the Knut and Alice Wallenberg Foundation and the EXSELENT Project, Sweden.

■ REFERENCES

(1) (a) Schattl, W. *Adv. Mater.* **2000**, *12*, 1899. (b) Caruso, F. *Adv. Mater.* **2001**, *13*, 11.

(2) (a) Yang, H. G.; Zeng, H. C. *Angew. Chem., Int. Ed.* **2004**, *43*, 5930. (b) Gao, P. X.; Wang, Z. L. *J. Am. Chem. Soc.* **2003**, *125*, 11299. (c) Jiang, Z. Y.; Xie, Z. X.; Zhang, X. H.; Lin, S. C.; Xu, T.; Xie, S. Y.; Huang, R. B.; Zheng, L. S. *Adv. Mater.* **2004**, *16*, 904. (d) Cao, H.; Qian, X.; Wang, C.; Ma, X.; Jin, X.; Zhu, Z. *J. Am. Chem. Soc.* **2005**, *127*, 16024.

(3) (a) Kresge, C. T.; Leonowicz, M. E.; Roth, W. J.; Vartuli, J. C.; Beck, J. S. *Nature* **1992**, *359*, 710. (b) Yanagisawa, T.; Shimizu, T.; Kuroda, K.; Kato, C. *Bull. Chem. Soc. Jpn.* **1990**, *63*, 988.

(4) Huo, Q.; Margolese, D. I.; Ciesla, U.; Demuth, D. G.; Feng, P.; Gier, T. E.; Sieger, P.; Firouzi, A.; Chmelka, B. F.; Schüth, F.; Stucky, G. D. *Chem. Mater.* **1994**, *6*, 1176.

(5) (a) Huo, Q.; Margolese, D. I.; Ciesla, U.; Feng, P.; Gier, T. E.; Sieger, P.; Leon, R.; Stucky, G. D. *Nature* **1994**, *368*, 317. (b) Huo, Q.; Leon, R.; Petroff, P. M.; Stucky, G. D. *Science* **1995**, *268*, 1324. (c) Tanev, P. T.; Pinnavaia, T. J. *Science* **1995**, *267*, 865. (d) Zhao, D.; Feng, J.; Huo, Q.; Melosh, N.; Fredrickson, G. H.; Chmelka, B. F.; Stucky, G. D. *Science* **1998**, *279*, 548. (e) Zhao, D.; Huo, Q.; Feng, J.; Chmelka, B. F.; Stucky, G. D. *J. Am. Chem. Soc.* **1998**, *120*, 6024. (f) Sakamoto, Y.; Kaneda, M.; Terasaki, O.; Zhao, D.; Kim, J. M.; Stucky, G. D.; Shin, H. J.; Ryoo, R. *Nature* **2000**, *408*, 449. (g) Yu, C.; Tian, B.; Fan, J.; Stucky, G. D.; Zhao, D. *J. Am. Chem. Soc.* **2002**, *124*, 4556. (h) Han, Y.; Zhang, D.; Chng, L. L.; Sun, J.; Zhao, L.; Zou, X.; Ying, J. Y. *Nat. Chem.* **2009**, *1*, 123.

(6) (a) Kim, J. M.; Kim, S. K.; Ryoo, R. *Chem. Commun.* **1998**, 259. (b) Guan, S.; Inagaki, S.; Ohsuna, T.; Terasaki, O. *J. Am. Chem. Soc.* **2000**, *122*, 5660. (c) Terasaki, O.; Ohsuna, T.; Liu, Z.; Sakamoto, Y.; Garcia-Bennett, A. E. *Stud. Surf. Sci. Catal.* **2004**, *148*, 261. (d) Che, S.; Kamiya, S.; Terasaki, O.; Tatsumi, T. *J. Am. Chem. Soc.* **2001**, *123*, 12089. (e) Kamiya, S.; Tanaka, H.; Che, S.; Tatsumi, T.; Terasaki, O. *Solid State Sci.* **2003**, *5*, 197. (f) Che, S.; Li, H.; Lim, S.; Sakamoto, Y.; Terasaki, O.; Tatsumi, T. *Chem. Mater.* **2005**, *17*, 4103. (g) Che, S.; Lim, S. H.; Kaneda, M.; Yoshitake, H.; Terasaki, O.; Tatsumi, T. *J. Am. Chem. Soc.* **2002**, *124*, 13962. (h) Yu, C.; Tian, B.; Fan, J.; Stucky, G. D.; Zhao, D. *J. Am. Chem. Soc.* **2002**, *124*, 4556.

(7) (a) Schacht, S.; Huo, Q.; Voigt-Martin, I. G.; Stucky, G. D.; Schüth, F. *Science* **1996**, *273*, 768. (b) Sun, Q.; Kooyman, P. J.; Grossmann, J. G.; Bomans, P. H. H.; Frederik, P. M.; Magusin, P. C. M. M.; Beelen, T. P. M.; van Santen, R. A.; Sommerdijk, N. A. J. M. *Adv. Mater.* **2003**, *15*, 1097. (c) Wang, J.; Xiao, Q.; Zhou, H.; Sun, P.; Yuan, Z.; Li, B.; Ding, D.; Shi, A.-C.; Chen, T. *Adv. Mater.* **2006**, *18*, 3284. (d) Li, Y.; Shi, J.; Hua, Z.; Chen, H.; Ruan, M.; Yan, D. *Nano Lett.* **2003**, *3*, 609.

(8) (a) Djojoputro, H.; Zhou, X. F.; Qiao, S. Z.; Wang, L. Z.; Yu, C. Z.; Lu, G. Q. *J. Am. Chem. Soc.* **2006**, *128*, 6320. (b) Wang, J.-G.; Li, F.; Zhou, H.-J.; Sun, P.-C.; Ding, D.-T.; Chen, T.-H. *Chem. Mater.* **2009**, *21*, 612.

(9) Che, S.; Garcia-Bennett, A. E.; Yokoi, T.; Sakamoto, K.; Kunieda, H.; Terasaki, O.; Tatsumi, T. *Nat. Mater.* **2003**, *2*, 801.

(10) Gao, C.; Sakamoto, Y.; Sakamoto, K.; Terasaki, O.; Che, S. *Angew. Chem., Int. Ed.* **2006**, *45*, 4295.

(11) Ino, S. *J. Phys. Soc. Jpn.* **1966**, *21*, 346.

(12) Lim, B.; Jiang, M.; Tao, J.; Camargo, P. H. C.; Zhu, Y.; Xia, Y. *Adv. Funct. Mater.* **2009**, *19*, 189.

(13) (a) Miyasaka, K.; Han, L.; Che, S.; Terasaki, O. *Angew. Chem., Int. Ed.* **2006**, *45*, 6516. (b) Han, L.; Sakamoto, Y.; Terasaki, O.; Li, Y.; Che, S. *J. Mater. Chem.* **2007**, *17*, 1216.

(14) Mader, S. *J. Vac. Sci. Technol.* **1966**, *8*, 247.

(15) Israelachvili, J. N.; Mitchell, D. J.; Ninham, B. W. *J. Chem. Soc., Faraday Trans. 2* **1976**, *72*, 1525.

(16) Quina, F. H.; Hinze, W. L. *Ind. Eng. Chem. Res.* **1999**, *38*, 4150.

(17) (a) Garcia-Bennett, A. E.; Lund, K.; Terasaki, O. *Angew. Chem., Int. Ed.* **2006**, *45*, 2434. (b) Han, L.; Chen, Q.; Wang, Y.; Gao, C.; Che, S. *Microporous Mesoporous Mater.* **2011**, *139*, 94.

(18) (a) Yang, H.; Coombs, N.; Ozin, G. A. *Nature* **1997**, *386*, 692. (b) Dabbs, D. M.; Aksay, I. A. *Annu. Rev. Phys. Chem.* **2000**, *51*, 601.

(19) Squires, A.; Templer, R. H.; Seddon, J. M.; Woenckhaus, J.; Winter, R.; Finet, S.; Theyencheri, N. *Langmuir* **2002**, *18*, 7384.

(20) (a) Jong, N.; Cate, F. J. T. *Ultrasonics* **1996**, *34*, 587. (b) Wheatley, A. M.; Forsberg, F.; Oum, K.; Ro, R.; EI-Sherif, D. *Ultrasonics* **2006**, *44*, 360.

(21) Lin, P.-L.; Eckersley, R. J.; Hall, E. A. H. *Adv. Mater.* **2009**, *21*, 1.